UDC 539.3
Doi: 10.31772/2587-6066-2020-21-4-499-513

For citation: Sabirov R. A. Compound bending of an orthotropic plate. *Siberian Journal of Science and Technology.* 2020, Vol. 21, No. 4, P. 499–513. Doi: 10.31772/2587-6066-2020-21-4-499-513

Для цитирования: Сабиров Р. А. Сложный изгиб ортотропной пластины // Сибирский журнал науки и технологий. 2020. Т. 21, № 4. С. 499–513. Doi: 10.31772/2587-6066-2020-21-4-499-513

COMPOUND BENDING OF AN ORTHOTROPIC PLATE

R. A. Sabirov

Reshetnev Siberian State University of Science and Technology
31, Krasnoyarskii rabochii prospekt, Krasnoyarsk, 660037, Russian Federation
E-mail: rashidsab@mail.ru

The problem of longitudinal-transverse deformation and strength of an orthotropic plate on the action of a local transverse force and stretching along the contour of the membrane forces is studied. The direction of laying the fiber of a unidirectional composite that provides the lowest level of stress and deflection is determined.

In the zone of application of concentrated force in thin-walled structures, significant bending moments and shear forces occur, which are a source of stress concentration. To reduce stresses, the method of plate tension by membrane forces applied along the contour is chosen. The maximum possible order of membrane tension forces is selected, which provides conditions for the strength and rigidity of the solar panel plate structure, which has a hinge-fixed support along the contour. Pre-tensioning the plate web allows to reduce the stress by 50 times.

The problem of compound bending of isotropic and anisotropic plates when applying transverse and selection of longitudinal loads, with restrictions on strength and stiffness, can be called a problem of rational design of the structure. The resulting equations and calculation program can be used in the design of plate structures, as well as in the educational process.

Keywords: plate bending, longitudinal-transverse deformation.

СЛОЖНЫЙ ИЗГИБ ОРТОТРОПНОЙ ПЛАСТИНЫ

Р. А. Сабиров

Сибирский государственный университет науки и технологий имени академика М. Ф. Решетнева
Российская Федерация, 660037, г. Красноярск, просп. им. газ. «Красноярский рабочий», 31
E-mail: rashidsab@mail.ru

Изучается вопрос продольно-поперечного деформирования и прочности ортотропной пластины от воздействия локальной поперечной силы и растягивающих по контуру мембранных сил. Определено направление укладки волокна однонаправленного композита, обеспечивающего наиболее низкий уровень напряжений и прогиба.

В зоне приложения сосредоточенной силы в тонкостенных конструкциях возникают существенные изгибающие моменты и перерезывающие силы, являющиеся источником концентрации напряжений. Для уменьшения напряжений выбран прием натяжения пластины мембранными силами, приложенными по контуру. Подобран максимально возможный порядок мембранных сил натяжения, обеспечивающий условия прочности и жесткости конструкции пластины солнечной батареи, имеющей шарнирно-неподвижное опирание по контуру. Предварительное натяжение полотна пластины позволяет уменьшить напряжения в 50 раз.

Задачу сложного изгиба изотропных и анизотропных пластин при приложении поперечных и подборе продольных нагрузок с ограничениями прочности и жесткости можно назвать задачей рационального проектирования конструкции. Полученные уравнения и программа расчета могут быть использованы как при проектировании конструкций пластин, так и в учебном процессе.

Ключевые слова: изгиб пластины, продольно-поперечное деформирование.

Introduction. Space technology uses rectangular flexible plates with photovoltaic cells attached to its surface. Plates are attached to rigid ribs and pre-stretched using forces in its plane [1; 2].

Composites, often unidirectional, the physical properties of which sometimes differ 15 times, and the strength differ up to 40 times are used [3] as materials. Therefore, the plate material should be considered substantially

orthotropic. The task is to ensure the fulfillment of the required conditions for the rigidity and strength of the plate.

A pre-stretched plate (membrane) is subjected to a transverse load, which is classified under the concept of compound bending [4]. In compound bending, as in simple bending, we can consider the total action on the plate of a number of different transverse loads, equal to the sum of the actions on it of all loads separately, however, if the membrane forces themselves are functions of the transverse load, then the principle of additivity (superposition) does not apply [5].

The transverse loads acting on the plate are distributed over a substantially small surface. When calculating structures, real loads are replaced by idealized forces, dividing them into loads distributed over a large surface, and local loads acting in a small area. When the dimensions of the zone within which the load acts are significantly small compared to the dimensions of the entire surface of the structure, or, for example, when the diameter of the loaded zone is less than the thickness of the plate, the load can be considered as local, applied at one point [6]. In the area of application of a concentrated force in thin-walled structures, significant bending moments and shearing forces arise. These local forces are the source of stress concentration. One of the methods for reducing stresses can be the tension of the plate by membrane forces applied along the contour.

On the theory of compound bending of isotropic plates, the following works can be mentioned [7–9]; a review and analysis of deformation models is given in [10–16].

Work objective. It is required to choose a model for calculating thin plates from an orthogonal anisotropic material; to solve the problem of ensuring the rigidity and strength of a compound bending of an orthotropic plate for optimal orientation of the composite fibers located in a rectangular non-deformable contour, with a simultaneous application of transverse and longitudinal loads.

I. Statement of the problem of deformation of an orthotropic model of compound bending. A differential formulation of the problem of longitudinal-transverse bending of a plate is considered. Geometric nonlinear equations are simplified: they neglect the derivatives of the functions of membrane displacements of the basal surface. The resolving equilibrium equation is compiled according to the deformed scheme.

1. Physical equations. As the governing equations, we use Hooke's law for a body with orthogonal-anisotropic properties, compiled in the Cartesian coordinate system *Oxyz* [17]

$$\begin{Bmatrix} \varepsilon_{xx} \\ \varepsilon_{yy} \\ \varepsilon_{xy} \end{Bmatrix} = \begin{bmatrix} c_{11} & c_{12} & 0 \\ c_{12} & c_{22} & 0 \\ 0 & 0 & c_{66} \end{bmatrix} \begin{Bmatrix} \sigma_x \\ \sigma_y \\ \tau_{xy} \end{Bmatrix}, \qquad (1)$$

where the components of the strain tensor ε_{xx}, ε_{yy}, ε_{xy} related to the stress tensor components σ_x, σ_y, τ_{xy} compliance coefficients:

$$c_{11} = 1/E_1, \quad c_{22} = 1/E_2, \quad c_{12} = -\nu_{21}/E_2,$$

$$c_{21} = -\nu_{12}/E_1, \; c_{66} = 1/G_{12}, \; (E_1\nu_{21} = E_2\nu_{12}). \qquad (2)$$

Here E_1, E_2, ν_{12}, ν_{21}, G_{12} are elastic characteristics of rigidity (technical constants) of an orthotropic material determined for the principal directions of elastic symmetry *1–2*.

The inverse matrix of (1) matrix has the form:

$$\begin{Bmatrix} \sigma_x \\ \sigma_y \\ \tau_{xy} \end{Bmatrix} = \begin{bmatrix} b_{11} & b_{12} & 0 \\ b_{12} & b_{22} & 0 \\ 0 & 0 & b_{66} \end{bmatrix} \begin{Bmatrix} \varepsilon_{xx} \\ \varepsilon_{yy} \\ \varepsilon_{xy} \end{Bmatrix}. \qquad (3)$$

Here,

$$b_{11} = \frac{c_{22}}{c_{11}c_{22} - c_{12}^2}, \qquad b_{12} = b_{21} = -\frac{c_{12}}{c_{11}c_{22} - c_{12}^2},$$

$$b_{22} = \frac{c_{11}}{c_{11}c_{22} - c_{12}^2}, \qquad b_{66} = \frac{1}{c_{66}}. \qquad (4)$$

The coefficients of matrix (3), expressed in terms of technical constants (2), have the form:

$$\begin{Bmatrix} \sigma_x \\ \sigma_y \\ \tau_{xy} \end{Bmatrix} = \begin{bmatrix} \dfrac{E_1}{1-\nu_{12}\nu_{21}} & \dfrac{\nu_{21}E_1}{1-\nu_{12}\nu_{21}} & 0 \\ \dfrac{\nu_{12}E_2}{1-\nu_{12}\nu_{21}} & \dfrac{E_2}{1-\nu_{12}\nu_{21}} & 0 \\ 0 & 0 & G_{12} \end{bmatrix} \begin{Bmatrix} \varepsilon_{xx} \\ \varepsilon_{yy} \\ \varepsilon_{xy} \end{Bmatrix}. \qquad (5)$$

2. Geometric equations (deformations). We apply the geometrically nonlinear Love – Karman – Novozhilov – Papkovich equations [4; 7; 10]:

$$\varepsilon_{xx} = \frac{\partial u_0}{\partial x} + \frac{1}{2}\left(\frac{\partial w}{\partial x}\right)^2 - \frac{\partial^2 w}{\partial x^2} z, \qquad (6)$$

$$\varepsilon_{yy} = \frac{\partial v_0}{\partial y} + \frac{1}{2}\left(\frac{\partial w}{\partial y}\right)^2 - \frac{\partial^2 w}{\partial y^2} z, \qquad (7)$$

$$\varepsilon_{xy} = \frac{\partial u_0}{\partial y} + \frac{\partial v_0}{\partial x} + \frac{\partial w}{\partial x}\frac{\partial w}{\partial y} - 2\frac{\partial^2 w}{\partial x \partial y} z. \qquad (8)$$

In practical plate design, membrane displacements $u_0 = u(x, y)$, $v_0 = v(x, y)$ one to two orders of magnitude less deflections of the middle layer $w = w(x, y)$. Therefore, in equations (6)–(7), we can exclude the derivatives of membrane displacement functions, which gives:

$$\varepsilon_{xx} = \frac{1}{2}\left(\frac{\partial w}{\partial x}\right)^2 - \frac{\partial^2 w}{\partial x^2} z, \qquad (9)$$

$$\varepsilon_{yy} = \frac{1}{2}\left(\frac{\partial w}{\partial y}\right)^2 - \frac{\partial^2 w}{\partial y^2} z, \qquad (10)$$

$$\varepsilon_{xy} = \frac{\partial w}{\partial x}\frac{\partial w}{\partial y} - 2\frac{\partial^2 w}{\partial x \partial y} z. \qquad (11)$$

Equations (9)–(11) can be called quasi-nonlinear, since they contain squares and the product of the first derivatives of the deflection functions.

3. Stress and internal strength factors. Substituting (9)–(11) in (3), we obtain the stress values:

$$\sigma_x(x,y,z)=b_{11}\left[\frac{1}{2}\left(\frac{\partial w}{\partial x}\right)^2-z\frac{\partial^2 w}{\partial x^2}\right]+$$

$$+b_{12}\left[\frac{1}{2}\left(\frac{\partial w}{\partial y}\right)^2-z\frac{\partial^2 w}{\partial y^2}\right], \quad (12)$$

$$\sigma_y(x,y,z)=b_{12}\left[\frac{1}{2}\left(\frac{\partial w}{\partial x}\right)^2-z\frac{\partial^2 w}{\partial x^2}\right]+$$

$$+b_{22}\left[\frac{1}{2}\left(\frac{\partial w}{\partial y}\right)^2-z\frac{\partial^2 w}{\partial y^2}\right], \quad (13)$$

$$\tau_{xy}(x,y,z)=b_{66}\left(\frac{\partial w}{\partial x}\frac{\partial w}{\partial y}-2\frac{\partial^2 w}{\partial x\partial y}z\right). \quad (14)$$

Integration of stresses (12)–(14) along the plate height h $(-h/2\le z\le h/2)$ gives a group of internal force factors, membrane forces, bending moments and torque:

$$N_x=\frac{h}{2}\left[b_{11}\left(\frac{\partial w}{\partial x}\right)^2+b_{12}\left(\frac{\partial w}{\partial y}\right)^2\right], \quad (15)$$

$$N_y=\frac{h}{2}\left[b_{12}\left(\frac{\partial w}{\partial x}\right)^2+b_{22}\left(\frac{\partial w}{\partial y}\right)^2\right], \quad (16)$$

$$S_{xy}=b_{66}h\frac{\partial w}{\partial x}\frac{\partial w}{\partial y}, \quad (17)$$

$$M_x=-\frac{h^3}{12}\left(b_{11}\frac{\partial^2 w}{\partial x^2}+b_{12}\frac{\partial^2 w}{\partial y^2}\right), \quad (18)$$

$$M_y=-\frac{h^3}{12}\left(b_{12}\frac{\partial^2 w}{\partial x^2}+b_{22}\frac{\partial^2 w}{\partial y^2}\right), \quad (19)$$

$$H_{xy}=-2b_{66}\frac{h^3}{12}\frac{\partial^2 w}{\partial x\partial y}. \quad (20)$$

4. Equilibrium equation. The model of S. P. Timoshenko, in which the equilibrium equation [9] corresponds to the state of compound bending:

$$\frac{\partial^2 M_x}{\partial x^2}+2\frac{\partial^2 H_{xy}}{\partial x^2}+\frac{\partial^2 M_y}{\partial y^2}=$$

$$=-q_z-N_x\frac{\partial^2 w}{\partial x^2}-N_y\frac{\partial^2 w}{\partial y^2}-2S_{xy}\frac{\partial^2 w}{\partial x\partial y}. \quad (21)$$

Substituting moments (18)–(20) into (21), we obtain the resolving equation for calculating the orthotropic plate

$$B_{11}\frac{\partial^4 w}{\partial x^4}+B_{12}\frac{\partial^4 w}{\partial x^2\partial y^2}+B_{22}\frac{\partial^4 w}{\partial y^4}=$$

$$=q_z+N_x\frac{\partial^2 w}{\partial x^2}+N_y\frac{\partial^2 w}{\partial y^2}+2S_{xy}\frac{\partial^2 w}{\partial x\partial y}, \quad (22)$$

in which the stiffness parameters are equal:

$$B_{11}=\frac{b_{11}h^3}{12},\quad B_{12}=\frac{2b_{12}+4b_{66}}{12}h^3,\quad B_{22}=\frac{b_{22}h^3}{12}. \quad (23)$$

In the right part (22) $N_x=N_x(x,y)$, $N_y=N_y(x,y)$ и $S_{xy}=S_{xy}(x,y)$. At the first step of calculating a compound bend, these forces are assumed to be equal to the pretensioning forces. It can be assumed that if in the numerical analysis of the plate deformation it turns out that the forces calculated by formulas (15)–(17), depending only on the squares of the first derivatives of the deflection functions, will be comparable with the order of the applied membrane tension forces, then the calculation problem should be reformulated and considered as a boundary value problem with variable coefficients.

5. Transition from a continuous problem statement to a discrete (finite-difference) one. Discretization of equations (22) is carried out by the method of grids [18], replacing the differential operators with central differences. Finite-difference analogue of differential equation (22) for a uniform square grid $i=1,2,...,n$, $j=1,2,...,m$, with step λ is the following:

$$\left[\frac{6(B_{11}+B_{22})+4B_{12}}{\lambda^4}+\frac{2(N_x+N_y)}{\lambda^2}\right]w_{i,j}-$$
$$-\left(\frac{4B_{11}+2B_{22}}{\lambda^4}+\frac{N_x}{\lambda^2}\right)w_{i,j+1}-\left(\frac{4B_{11}+2B_{22}}{\lambda^4}+\frac{N_x}{\lambda^2}\right)w_{i,j-1}-$$
$$-\left(\frac{4B_{22}+2B_{12}}{\lambda^4}+\frac{N_y}{\lambda^2}\right)w_{i+1,j}-\left(\frac{4B_{22}+2B_{12}}{\lambda^4}+\frac{N_y}{\lambda^2}\right)w_{i-1,j}+$$
$$+\frac{B_{12}}{\lambda^4}w_{i+1,j+1}+\frac{B_{12}}{\lambda^4}w_{i+1,j-1}+\frac{B_{12}}{\lambda^4}w_{i-1,j-1}+$$
$$+\frac{B_{12}}{\lambda^4}w_{i-1,j+1}+\frac{B_{11}}{\lambda^4}w_{i,j+2}+\frac{B_{11}}{\lambda^4}w_{i,j-2}+$$
$$+\frac{B_{11}}{\lambda^4}w_{i+1,j}+\frac{B_{11}}{\lambda^4}w_{i-1,j}=\frac{P_{ij}}{\lambda^2}. \quad (24)$$

6. Internal force factors and stresses of a discrete problem. Internal force factors are calculated by the formulas (15)–(17):

$$N_x^{(i,j)}=$$
$$=\frac{h}{2}\left[b_{11}\left(\frac{w_{i,j+1}-w_{i,j-1}}{2\lambda_x}\right)^2+b_{12}\left(\frac{w_{i+1,j}-w_{i-1,j}}{2\lambda_y}\right)^2\right], \quad (25)$$

$$N_y^{(i,j)}=$$
$$=\frac{h}{2}\left[b_{12}\left(\frac{w_{i,j+1}-w_{i,j-1}}{2\lambda_x}\right)^2+b_{22}\left(\frac{w_{i+1,j}-w_{i-1,j}}{2\lambda_y}\right)^2\right], \quad (26)$$

$$S_{xy}^{(i,j)}=b_{66}h\frac{w_{i,j+1}-w_{i,j-1}}{2\lambda_x}\frac{w_{i+1,j}-w_{i-1,j}}{2\lambda_y}, \quad (27)$$

$$M_x^{(i,j)}=-\frac{h^3}{12}\left(b_{11}\frac{w_{i,j+1}-2w_{i,j}+w_{i,j-1}}{\lambda_x^2}+\right.$$
$$\left.+b_{12}\frac{w_{i+1,j}-2w_{i,j}+w_{i-1,j}}{\lambda_y^2}\right), \quad (28)$$

$$M_y^{(i,j)} = -\frac{h^3}{12}\left(b_{12}\frac{w_{i,j+1} - 2w_{i,j} + w_{i,j-1}}{\lambda_x^2} + \right.$$

$$\left. + b_{22}\frac{w_{i+1,j} - 2w_{i,j} + w_{i-1,j}}{\lambda_y^2} \right), \qquad (29)$$

$$H_{xy}^{(i,j)} = -2b_{66}\left(\frac{h^3}{12}\right)\frac{1}{4\lambda_x\lambda_y}\times$$

$$\times\left(w_{i+1,j+1} - w_{i-1,j+1} + w_{i-1,j-1} + w_{i+1,j-1}\right). \qquad (30)$$

Stresses are calculated at grid points: $\sigma_x^{\max} = \pm M_x / h^2$, $\sigma_y^{\max} = \pm M_y / h^2$, $\tau_{xy}^{\max} = \pm H_{xy} / h^2$.

II. Calculations of the stiffness and strength of an orthotropic plate. The longitudinal-transverse deformation of an anisotropic plate is considered, and the strength is estimated. The level of membrane forces is determined, depending only on the squares of the first derivatives of the deflection functions. The calculations were performed on the basis of our own Maple program [19].

1. Given. Let us consider a plate $(1\,m \times 0.8\,m)$ made of unidirectional carbon fiber reinforced plastic [3] Tornel-300 (Carbon-fiber-reinforced-polymer (CFRP)), thickness h = 2 mm. Strength of the material along the grain $\sigma_1^+ = 1400\,\text{MPa}$, across the grain $\sigma_2^+ = 34.5\,\text{MPa}$; shear strength $\tau_{12} = 74\,\text{MPa}$. Tensile modulus along fibers $E_1 = 142.8\,GPa$; tensile modulus across fibers $E_2 = 9.13\,GPa$; Poisson's ratios: $\nu_{21} = 0.32$, $\nu_{12} = 0.02$. Shear modulus is $G_{12} = 5.49\,GPa$. Maximum deflection boom $w^+ \le 15\ mm$.

The plate is exposed to concentrated force P = 1000N in the centre. A hinge-fixed support is specified along the contour.

2. Determination of the most favorable orientation of fibers of a unidirectional composite in terms of plate stiffness. Let us investigate the stress-strain state from the action of only a concentrated shear force P.

In fig. 1 let us consider the orientation of the composite in the global coordinate system of the plate (Oxy) and give the strength parameters with the stiffness characteristics in its own principal axes O12. Let's call these parameters and characteristics normative.

Let us show in fig. 2 options for the arrangement of fibers: we orient the composite of unidirectional CFRP with fibers parallel to the long side of the plate (fig. 2, *a*) and parallel to the short side of the plate (fig. 2, *b*).

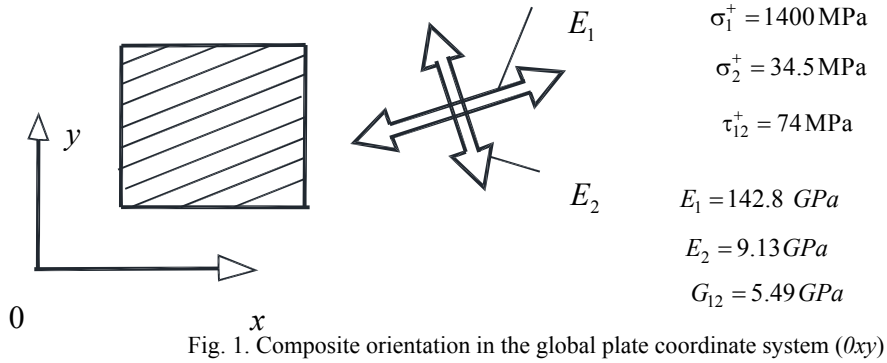

Fig. 1. Composite orientation in the global plate coordinate system (*0xy*) and strength parameters with stiffness characteristics

Рис. 1. Ориентация композита в глобальной системе координат пластины (*0xy*) и прочностные параметры с характеристиками жесткости

a *b*

Fig. 2. Plates with two types of composite fiber orientation: *a* – carbon fiber is located along the long side of the plate; *b* – carbon fiber is located along the short side of the plate

Рис. 2. Пластины с двумя видами ориентации волокон композита: *а* – волокна углепластика расположены вдоль длинной стороны пластины; *б* – волокна углепластика расположены вдоль короткой стороны пластины

Let us write the physical law for the first orientation of the fibers along the long side of the plate (fig. 2, *а*):

$$\begin{Bmatrix}\varepsilon_{xx}\\ \varepsilon_{yy}\\ \varepsilon_{xy}\end{Bmatrix}=\begin{bmatrix}\frac{1}{142.8\,GPa} & -\frac{0.02}{9.13\,GPa} & 0\\ -\frac{0,32}{142.8\,GPa} & \frac{1}{9.13\,GPa} & 0\\ 0 & 0 & \frac{1}{5.49\,GPa}\end{bmatrix}\begin{Bmatrix}\sigma_x\\ \sigma_y\\ \tau_{xy}\end{Bmatrix}$$

and for the second orientation of fibers along the short side of the plate (fig. 2, *б*):

$$\begin{Bmatrix}\varepsilon_{xx}\\ \varepsilon_{yy}\\ \varepsilon_{xy}\end{Bmatrix}=\begin{bmatrix}\frac{1}{9.13\,GPa} & -\frac{0,32}{142.8\,GPa} & 0\\ -\frac{0,02}{9.13\,GPa} & \frac{1}{142.8\,GPa} & 0\\ 0 & 0 & \frac{1}{5.49\,GPa}\end{bmatrix}\begin{Bmatrix}\sigma_x\\ \sigma_y\\ \tau_{xy}\end{Bmatrix}.$$

Let's perform the calculations, the results are shown in fig. 3–7.

The most favorable orientation of the fibers of a unidirectional composite in terms of plate rigidity is the arrangement of the composite fibers along its short side. In this case, the deflections are less by 56 % than when the fibers are arranged along the long side. Normal stresses in both cases are greater than the normative ones, strength is not ensured. Stress regulation is required. Calculations for both fiber arrangements are discussed below.

3. Location of composite fibers along the long side of the plate. The loads $N_x = 10^5\ N/m$ and $N_y = 10^5\ N/m$ are applies. The calculation results are shown in fig. 8. The initial stresses from pre-tension are equal to: $\sigma_x^0 = N_x / h$ и $\sigma_y^0 = N_y / h$.

The results shown in fig. 8, *а* show that under tension $N_x = 10^5\ N/m$ deflection in the center of the plate $w^{\max} = 20,8\,mm > w^+$ and stresses across the fibers, equal $\sigma_y^{\max} = 130\ \text{MPa} > \sigma_2^+$, are above standard.

The results shown in fig. 8, *b* show that under tension $N_y = 10^5\ N/m$ deflection in the center of the plate $w^{\max} = 10.05\,mm < w^+$, which satisfies the stiffness condition, and the stresses across the fibers $\sigma_y^{\max} = 129.8\,\text{MPa} > \sigma_2^+$ remain above standard.Let's increase efforts of N_x and N_y by an order. The calculation results are shown in fig. 9.

When loading the plate with pretension $N_x = 10^6\ N/m$ (fig. 9, *а*), the stress acting across the fibers decreases from 474,6 MPa (at $N_x = 0$) to 31,9 MPa (at $N_x = 10^6$ Н/м).

The applied force $N_y = 10^6\ N/m$ (fig. 9, *b*) by itself creates a preliminary tension across the fibers significantly more than the standard $\sigma_y^0 = 500\,\text{MPa} > \sigma_2^+$. As for the deflection, it is significantly less than the standard and equal to $w^{\max} = 1.84\,mm < w^+$.

Let us present the diagrams of deflection and internal force factors for this loading case in fig. 10–14.

4. Location of composite fibers along the short side of the plate. The loads $N_x = 10^5\ N/m$ and $N_y = 10^5\ N/m$ are applied. The calculation results are shown in fig. 13. The initial stresses from pre-tension are equal to: $\sigma_x^0 = N_x / h$ и $\sigma_y^0 = N_y / h$.

The results presented in fig. 13 *а* show that when stretched by force $N_x = 10^5\ N/m$ deflection in the center of the plate $w^{\max} = 11,3\,mm < w^+$ turned out to be of the same order of magnitude with the allowable deflection, and the stresses across the fibers, it is $\sigma_x^{\max} = 130.9\ \text{MPa} > \sigma_2^+$, above the standard.

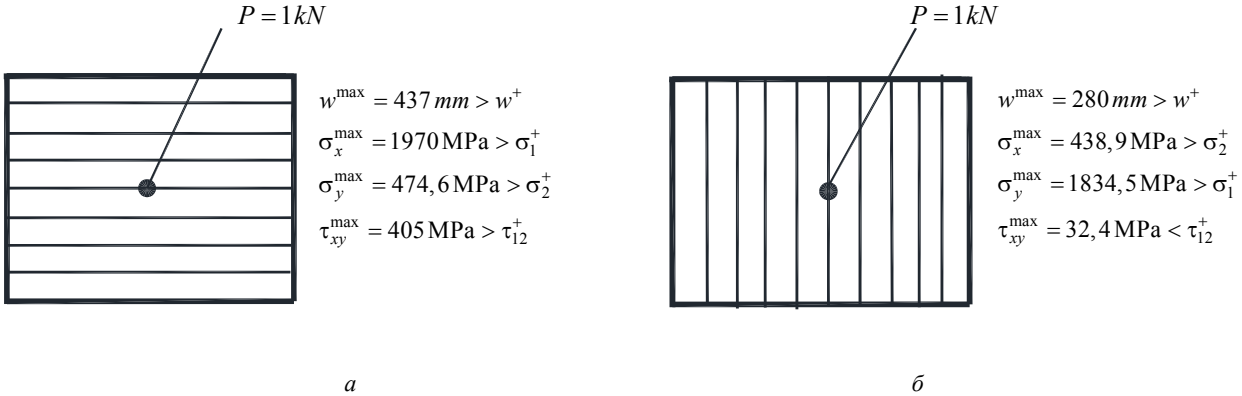

а *б*

Fig. 3. Comparison of deflections and maximum stresses with standard:
а – fiber CFRP along the long sides of the plate; *b* – CFRP fibers are located along the short sides of the plate

Рис. 3. Сравнение прогибов и максимальных напряжений с нормативными:
а – волокна углепластика расположены вдоль длинной стороны пластины;
б – волокна углепластика расположены вдоль короткой стороны пластины

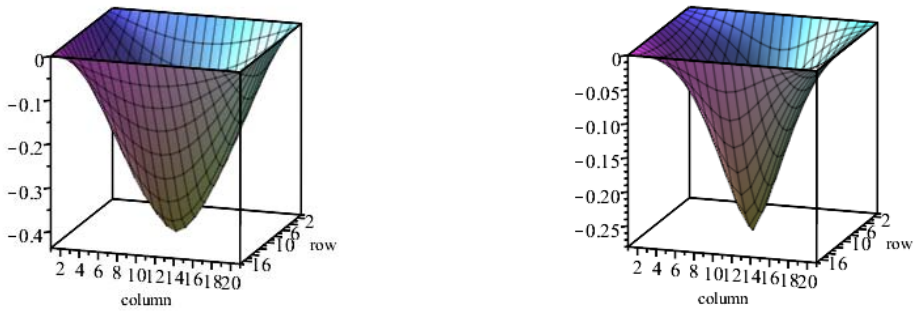

а *б*

Fig. 4. Comparison plots of deflections:
a – fiber CFRP along the long sides of the plate; *b* – CFRP fibers are located along the short sides of the plate

Рис. 4. Сравнение эпюр прогибов:
а – волокна углепластика расположены вдоль длинной стороны пластины;
б – волокна углепластика расположены вдоль короткой стороны пластины

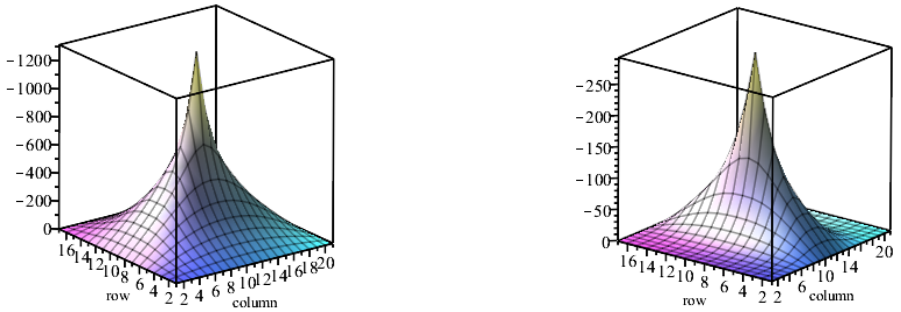

а *б*

Fig. 5. Comparison of bending moments M_x:
a – CFRP fibers are located along the long side of the plate;
b – CFRP fibers are located along the short side of the plate

Рис. 5. Сравнение изгибающих моментов M_x:
а – волокна углепластика расположены вдоль длинной стороны пластины;
б – волокна углепластика расположены вдоль короткой стороны пластины

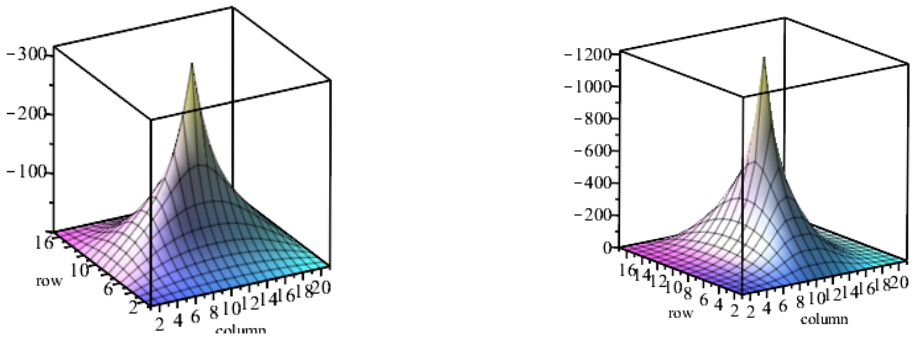

а *б*

Fig. 6. Comparison of bending moments M_y:
a – CFRP fibers are located along the long side of the plate;
b – CFRP fibers are located along the short sides of the plate

Рис. 6. Сравнение изгибающих моментов M_y:
а – волокна углепластика расположены вдоль длинной стороны пластины;
б – волокна углепластика расположены вдоль короткой стороны пластины

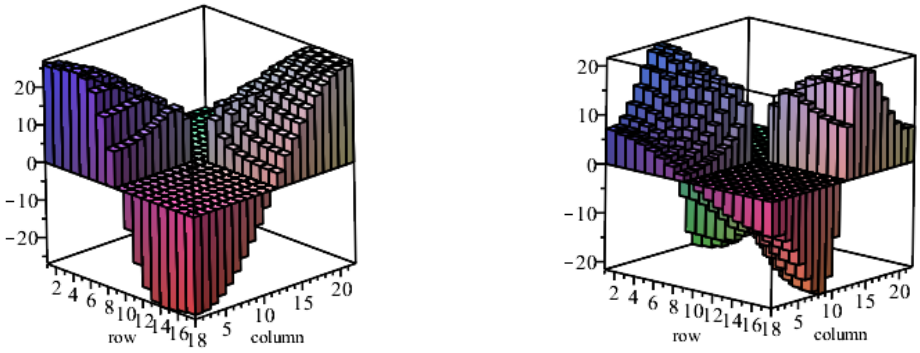

а *б*

Fig. 7. Comparison of torque H_{xy}:
a – CFRP fibers are located along the long side of the plate;
b – CFRP fibers are located along the short sides of the plate

Рис. 7. Сравнение крутящих моментов H_{xy}:
а – волокна углепластика расположены вдоль длинной стороны пластины;
б – волокна углепластика расположены вдоль короткой стороны пластины

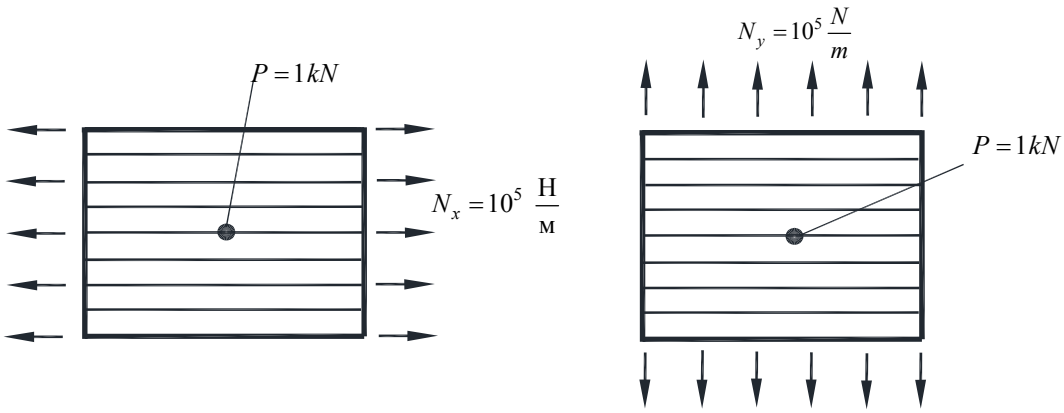

$w^{\max} = 20.8\,mm > w^+$
$\sigma_x^0 = 50\,\text{MPa} < \sigma_1^+$
$\sigma_y^0 = 0$
$\sigma_x^{\max} = 559\ \text{MPa} < \sigma_1^+$
$\sigma_y^{\max} = 130\ \text{MPa} > \sigma_2^+$
$\tau_{xy}^{\max} = 5.65\ \text{MPa} < \tau_{12}^+$

$w^{\max} = 10.05\,mm < w^+$
$\sigma_x^0 = 0$
$\sigma_y^0 = 50\,\text{MPa} > \sigma_2^+$
$\sigma_x^{\max} = 374.0\ \text{MPa} < \sigma_1^+$
$\sigma_y^{\max} = 129.8\ \text{MPa} > \sigma_2^+$
$\tau_{xy}^{\max} = 3.8\ \text{MPa} < \tau_{12}^+$

а *б*

Fig. 8. Calculation results for a plate in which CFRP fibers are located along its long side:
a – pre – stretching by force $N_x = 10^5$ N/m ; *b* – pre-stretching by force $N_y = 10^5$ N/m

Рис. 8. Результаты расчета пластины, в которой волокна углепластика расположены вдоль ее длинной стороны:
а – предварительное растяжение силой $N_x = 10^5$ Н/м ;
б – предварительное растяжение силой $N_y = 10^5$ Н/м

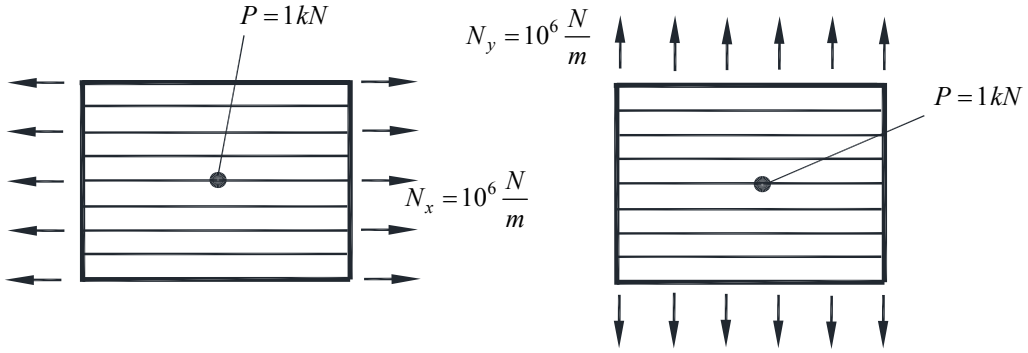

$w^{\max} = 3.72\,mm < w^+$
$\sigma_x^0 = 500\,\text{MPa} < \sigma_1^+$
$\sigma_y^0 = 0$
$\sigma_x^{\max} = 617\ \text{MPa} < \sigma_1^+$
$\sigma_y^{\max} = 31.9\ \text{MPa} < \sigma_2^+ = 34.5\ \text{MPa}$
$\tau_{xy}^{\max} = 0.96\ \text{MPa} < \tau_{12}^+$

а

$w^{\max} = 1.84\,mm < w^+$
$\sigma_x^0 = 0$
$\sigma_y^0 = 500\ \text{MPa} > \sigma_2^+$
$\sigma_x^{\max} = 121.6\ \text{MPa} < \sigma_1^+$
$\sigma_y^{\max} = 524.0\ \text{MPa} > \sigma_2^+$
$\tau_{xy}^{\max} = 0.76\ \text{MPa} < \tau_{12}^+$

б

Fig. 9. Results of calculating a plate in which CFRP fibers are located along its long side:
a – pre – stretching by force $N_x = 10^6$ N/m ; *b* – pre-stretching is applied $N_y = 10^6$ N/m

Рис. 9. Результаты расчета пластины, в которой волокна углепластика расположены вдоль ее длинной стороны:
а – предварительное растяжение силой $N_x = 10^6$ Н/м ;
б – приложено предварительное растяжение $N_y = 10^6$ Н/м

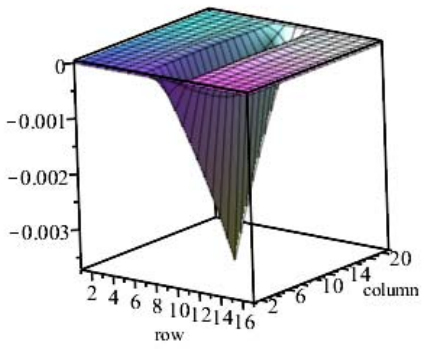

Fig. 10. Diagram of deflections for calculating a plate in which CFRP fibers are located along its long side $N_x = 10^6$ N/m and $P = 1\ kN$

Рис. 10. Эпюра прогибов расчета пластины, в которой волокна углепластика расположены вдоль ее длинной стороны при $N_x = 10^6$ Н/м и $P = 1$ кН

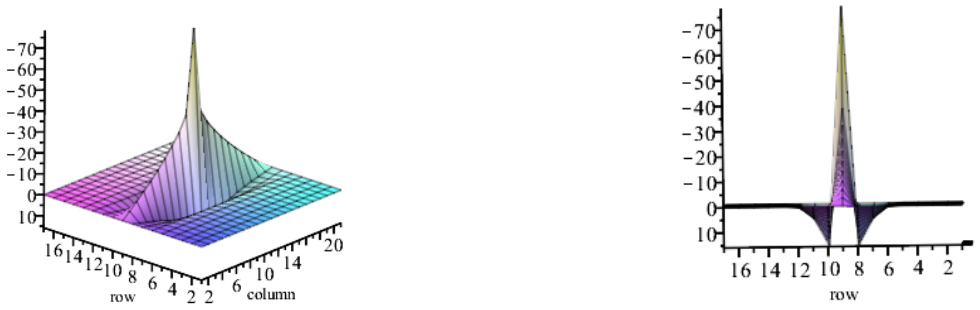

а *б*

Fig. 11. Diagram of the bending moment M_x of a plate in which CFRP fibers are located along its long side at $N_x = 10^6$ N/m and $P = 1$ *kN* :
a – general view of the diagram; *b* – view of the diagram in the *0yz* plane

Рис. 11. Эпюра изгибающего момента M_x, в которой волокна углепластика расположены вдоль длинной стороны при $N_x = 10^6$ Н/м и $P = 1$ кН :
а – общий вид эпюры; *б* – вид эпюры в плоскости *0yz*

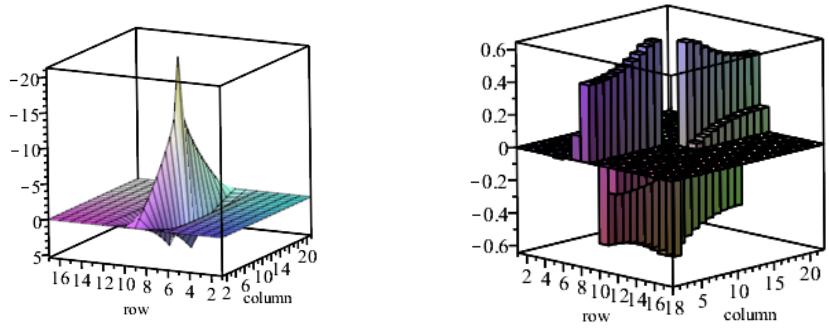

а *б*

Fig. 12. Diagrams of moments of a plate in which CFRP fibers are located along its long side at $N_x = 10^6$ N/m and $P = 1$ *kN* :
a – plot M_x; *b* – plot H_{xy}

Рис. 12. Эпюры моментов пластины, в которой волокна углепластика расположены вдоль ее длинной стороны при $N_x = 10^6$ Н/м и $P = 1$ кН :
а – эпюра M_x; *б* – эпюра H_{xy}

The results shown in fig. 13 *b* show that under tension $N_y = 10^5\ N/m$ in the center of the plate deflection $w^{\max} = 18{,}16\,mm > w^+ = 15\,mm$, that does not satisfy the stiffness condition; also the stress across the fibers, equal to $\sigma_x^{\max} = 127{,}7$ MPa $> \sigma_2^+$, is higher than the standard.

Let's increase forces N_x and N_y to an order of magnitude. The calculation results are shown in fig. 14.

The pre-tension by force $N_x = 10^6\,N/m$ gives tension across the fibers ($\sigma_x^0 = 500$ MPa $> \sigma_2^+$) more regulatory stress. The combined action of the shear force and the tensile force increased this stress ($\sigma_x^{\max} = 525.4$ MPa $> \sigma_2^+$).

When the plate is loaded (fig. 14, *a*) with a load acting across the fibers, the stress decreases from 474.6 MPa (at $N_x = 0$) to 31.9 MPa (at $N_x = 10^6\,N/m$).

Applied effort $N_y = 10^6\,N/m$ (fig. 14, *b*) meets all the criteria of rigidity and strength.

Let us present the diagrams of the deflection and internal force factors for this case of loading in fig. 15–17.

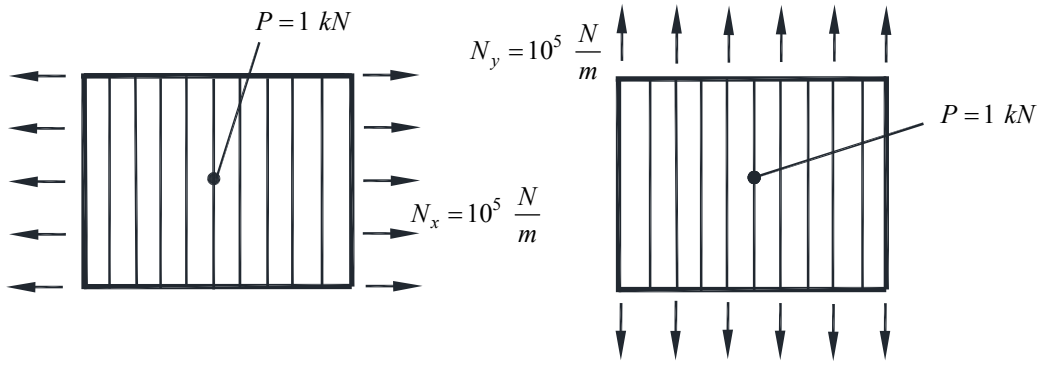

$w^{\max} = 11.3\ mm < w^+$
$\sigma_x^0 = 50\ \text{MPa} > \sigma_2^+$
$\sigma_y^0 = 0$
$\sigma_x^{\max} = 130.9\ \text{MPa} > \sigma_2^+$
$\sigma_y^{\max} = 378.7\ \text{MPa} < \sigma_1^+$
$\tau_{xy}^{\max} = 3,77\ \text{MPa} < \tau_{12}^+$

а

$w^{\max} = 18.16\,mm > w^+$
$\sigma_x^0 = 0$
$\sigma_y^0 = 50\ \text{MPa} < \sigma_1^+$
$\sigma_x^{\max} = 127.7\ \text{MPa} > \sigma_2^+$
$\sigma_y^{\max} = 552.0\ \text{MPa} < \sigma_1^+$
$\tau_{xy}^{\max} = 5.874\ \text{MPa} < \tau_{12}^+$

б

Fig. 13. Results of calculating a plate in which CFRP fibers are located along its short side:
A – pre – stretching is $N_x = 10^5$ N/m ; *b* – applied pre-stretching is $N_y = 10^5$ N/m

Рис. 13. Результаты расчета пластины, в которой волокна углепластика расположены вдоль ее короткой стороны:
а – предварительное растяжение $N_x = 10^5$ Н/м ;
б – приложено предварительное растяжение $N_y = 10^5$ Н/м

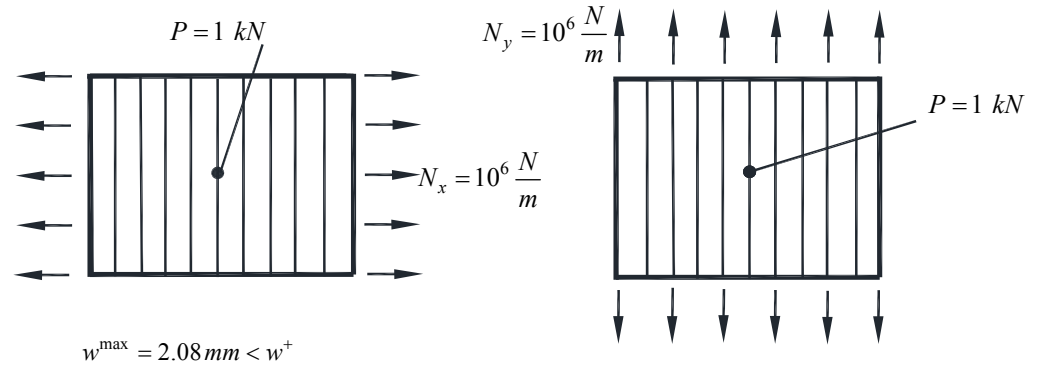

$w^{\max} = 2.08\,mm < w^+$
$\sigma_x^0 = 500\ \text{MPa} > \sigma_2^+$
$\sigma_y^0 = 0$
$\sigma_x^{\max} = 525.4\ \text{MPa} > \sigma_2^+$
$\sigma_y^{\max} = 124.9\ \text{MPa} < \sigma_1^+$
$\tau_{xy}^{\max} = 0.75\ \text{MPa} < \tau_{12}^+$

а

$w^{\max} = 3,18\ mm < w^+$
$\sigma_x^0 = 0$
$\sigma_y^0 = 500\ \text{MPa} < \sigma_1^+$
$\sigma_x^{\max} = 29.86\ \text{MPa} < \sigma_2^+ = 34.5\ \text{MPa}$
$\sigma_y^{\max} = 611.4\ \text{MPa} < \sigma_1^+$
$\tau_{xy}^{\max} = 0.97\ \text{MPa} < \tau_{12}^+$

б

Fig. 14. Results of calculating a plate in which CFRP fibers are located along its short side:
a – applied pre – tension is $N_x = 10^6$ N/m ; *b* – applied pre-tension is $N_y = 10^6$ N/m

Рис. 14. Результаты расчета пластины, в которой волокна углепластика расположены вдоль ее короткой стороны:
а – приложено предварительное растяжение $N_x = 10^6$ Н/м ;
б – приложено предварительное растяжение $N_y = 10^6$ Н/м

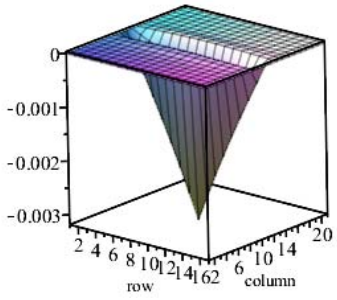

Fig. 15. Diagram of deflections of a plate in which CFRP fibers are located along its short side at $N_x = 10^6$ N/m and $P = 1$ *kN*

Рис. 15. Эпюра прогибов пластины, в которой волокна углепластика расположены вдоль ее короткой стороны при $N_x = 10^6$ Н/м и $P = 1$ кН

а *б*

Fig. 16. Diagrams of moments of a plate in which CFRP fibers are located along its short side of the short side at $N_y = 10^6$ N/m and $P = 1$ *kN* :

a – M_x; *b* – H_{xy}

Рис. 16. Эпюры моментов пластины, в которой волокна углепластика расположены вдоль ее короткой стороны короткой стороны при $N_y = 10^6$ Н/м и $P = 1$ кН :

а – M_x; *б* – H_{xy}

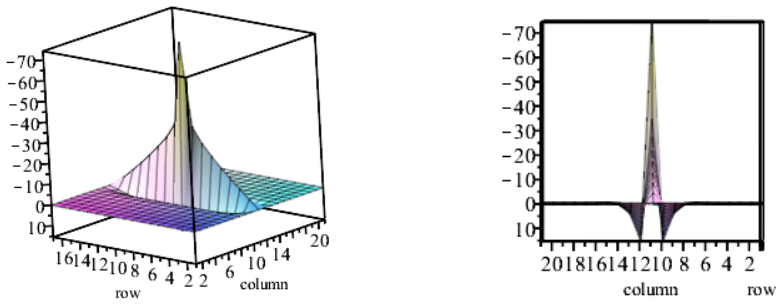

а *б*

Fig. 17. Diagrams of moments of a plate in which CFRP fibers are located along its short side at $N_y = 10^6$ N/m at and $P = 1$ *kN* :

a – general view; *b* – view in the *0xz* plane

Рис. 17. Эпюры моментов пластины, в которой волокна углепластика расположены вдоль ее короткой стороны при $N_y = 10^6$ Н/м и $P = 1$ кН :

а – общий вид; *б* – вид в плоскости *0xz*

According to the results of calculations of a plate reinforced along its long and short sides, it was found that, according to the required characteristics of rigidity and strength, both variants of tension by membrane forces are suitable N_x и N_y.

When reinforcing along the long side of the plate, the pretension by force $N_x = 10^6$ N/m reduces the stress acting along the fibers from 1970 MPa to 617 MPa (fig. 3, *a*), and the stress acting across the fibers, equal to 474.6 MPa, is reduced by the preliminary tension to 31.9 MPa (fig. 9, *a*).

For reinforcement on the short side, the pretension by force $N_y = 10^6 N/m$ reduces the stress acting across the fibers from 438 MPa to 29.86 MPa (fig. 3, *b*), and the stress acting along the fibers, equal to 1834.5 MPa, is reduced by the pretensioning to 611.44 MPa (fig. 14 *b*).

5. Simultaneous loading of plates with membrane forces N_x and N_y. In fig. 18 we present the results of calculating a plate in which the fibers of the composite are located along its long side (fig. 18, *a*), and a plate in which the fibers are located along its short side (fig. 18, *b*). In both cases, stretching by membrane forces is performed simultaneously by forces $N_x = 10^5 N/m$ and $N_y = 10^5 N/m$. Both types of loading do not satisfy the strength across the fibers. Let's increase the membrane tensile forces by 10 times (fig. 19).

Diagrams for a plate in which CFRP fibers are located along the short side of the plate are shown in fig. 20.

Both variants of loading the plates, in which the fibers are oriented both along the long and short sides, do not correspond to the strength across the fibers of the composite material. Therefore, it is necessary to select a material with increased strength in the direction of the anisotropy axis 2.

Stretching of a rectangular composite web simultaneously in two directions presents certain technological difficulties; therefore, this option of pretensioning should be abandoned.

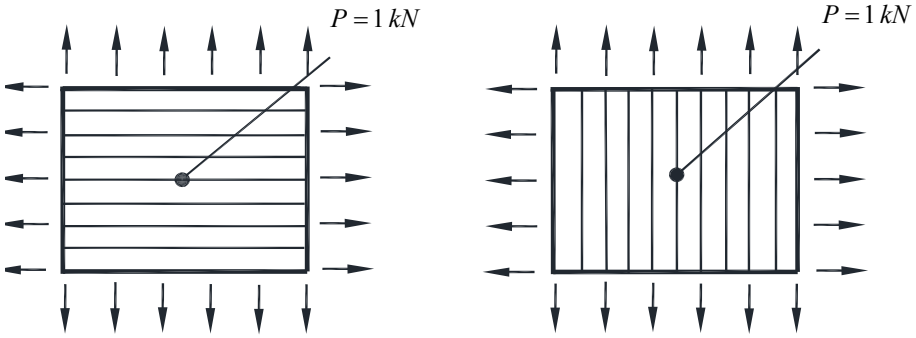

$w^{\max} = 5.25\,mm < w^+$
$\sigma_x^0 = 50$ MPa $< \sigma_1^+$
$\sigma_y^0 = 50$ MPa $> \sigma_2^+$
$\sigma_x^{\max} = 265.4$ MPa $< \sigma_1^+$
$\sigma_y^{\max} = 97.43$ MPa $> \sigma_2^+$
$\tau_{xy}^{\max} = 2.4$ MPa $< \tau_{12}^+$

а

$w^{\max} = 5.25\ mm < w^+$
$\sigma_x^0 = 50$ MPa $> \sigma_2^+$
$\sigma_y^0 = 50$ MPa $< \sigma_1^+$
$\sigma_x^{\max} = 97.6$ MPa $> \sigma_2^+$
$\sigma_y^{\max} = 265.9$ MPa $< \sigma_1^+$
$\tau_{xy}^{\max} = 2.4$ MPa $< \tau_{12}^+$

б

Fig. 18. Comparison of deflections and maximum stresses with standard ones when loads are applied simultaneously $N_x = 10^5$ N/m and $N_y = 10^5$ N/m:

a – CFRP fibers are located along the long side of the plate;
b – carbon fiber fibers are located along the short side of the plate

Рис. 18. Сравнение прогибов и максимальных напряжений с нормативными при одновременном приложении нагрузок $N_x = 10^5$ Н/м и $N_y = 10^5$ Н/м:

а – волокна углепластика расположены вдоль длинной стороны пластины;
б – волокна углепластика расположены вдоль короткой стороны пластины

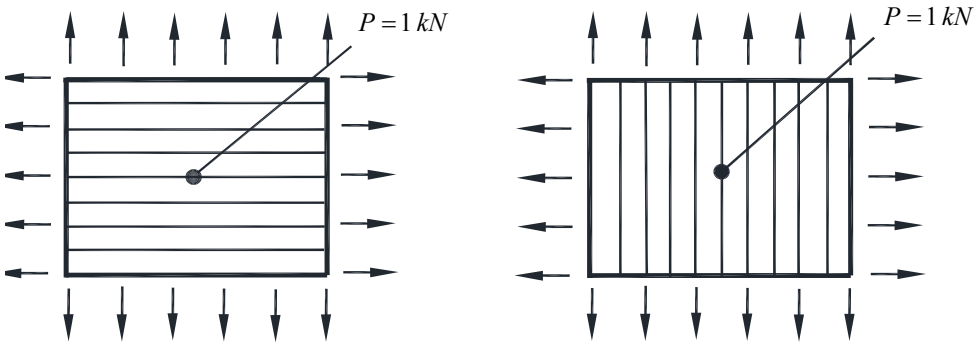

$w^{\max} = 0.60\ mm < w^{+}$
$\sigma_x^0 = 500\ \text{MPa} < \sigma_1^{+}$
$\sigma_y^0 = 500\ \text{MPa} > \sigma_2^{+}$
$\sigma_x^{\max} = 532.4\ \text{MPa} < \sigma_1^{+}$
$\sigma_y^{\max} = 506.9\ \text{MPa} > \sigma_2^{+}$
$\tau_{xy}^{\max} = 0.38\ \text{MPa} < \tau_{12}^{+}$

а

$w^{\max} = 0.60\ mm < w^{+}$
$\sigma_x^0 = 500\ \text{MPa} > \sigma_2^{+}$
$\sigma_y^0 = 500\ \text{MPa} < \sigma_1^{+}$
$\sigma_x^{\max} = 506.95\ \text{MPa} > \sigma_2^{+}$
$\sigma_y^{\max} = 532.1\ \text{MPa} < \sigma_1^{+}$
$\tau_{xy}^{\max} = 0.32\ \text{MPa} < \tau_{12}^{+}$

б

Fig. 19. Comparison of deflections and maximum stresses with standard ones when loads are applied simultaneously $N_x = 10^6$ N/m and $N_y = 10^6$ N/m:

a – CFRP fibers are located along the long side of the plate;
b – CFRP fibers are located along the short side of the plate

Рис. 19. Сравнение прогибов и максимальных напряжений с нормативными при одновременном приложении нагрузок $N_x = 10^6$ Н/м и $N_y = 10^6$ Н/м:

а – волокна углепластика расположены вдоль длинной стороны пластины;
б – волокна углепластика расположены вдоль короткой стороны пластины

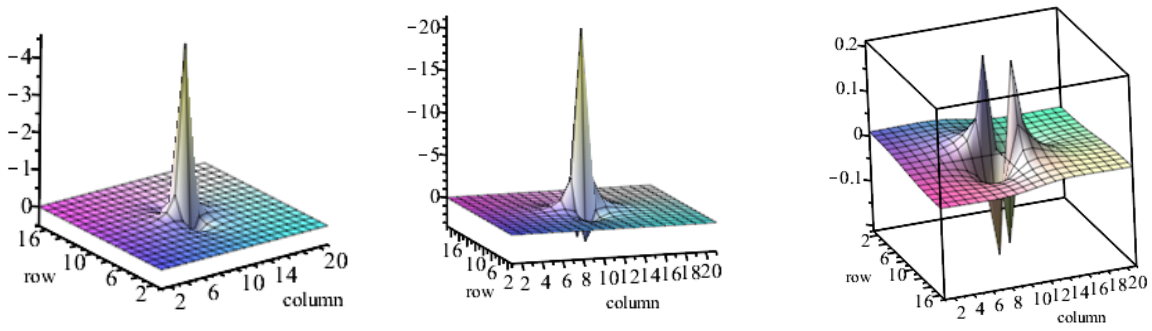

а *б* *с*

Fig. 20. Results of calculations of a plate in which CFRP fibers are located along the short side: *a* – moment M_x; *b* – moment M_x; *c* – moment H_{xy}

Рис. 20. Результаты вычислений пластины, в которой волокна углепластика расположены вдоль короткой стороны: *а* – момент M_x; *б* – момент M_x; *с* – момент H_{xy}

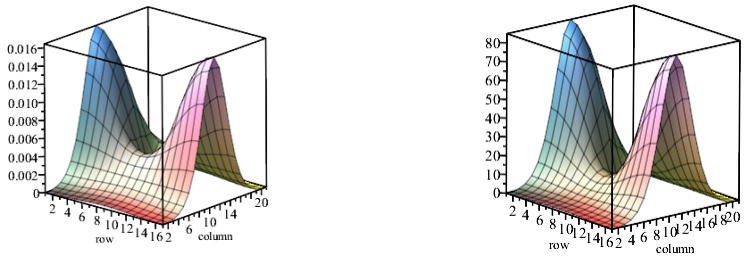

а *б*

Fig. 21. Diagrams of calculated longitudinal forces $N_x = N_x(x, y)$ and $N_y = N_y(x, y)$:

a – diagram N_x ; b – diagram N_y

Рис. 21. Эпюры вычисляемых продольных сил $N_x = N_x(x, y)$ и $N_y = N_y(x, y)$:

a – эпюра N_x ; $б$ – эпюра N_y

6. A numerical estimate of simplification of geometric equations of the boundary value problem. To estimate the level of efforts (15) and (16), which depend only on the squares of the first derivatives of the deflection functions, we consider the calculation data for an orthotropic plate. Compared with the specified longitudinal forces, the level of which was assigned from 10^5 to 10^6 N/m, which gives stresses of the order of 50 MPa to 500 MPa, the forces calculated by formulas (15) and (16) (fig. 21) give the maximum stresses up to 0.04 MPa. That is, the squares of the first derivatives of the deflection function $(\partial w / \partial x)^2$ and $(\partial w / \partial y)^2$ in (15) and (16) have little effect on the values of longitudinal membrane forces $N_x = N_x(x, y)$ and $N_y = N_y(x, y)$.

Thus, following the calculated results, it makes no sense to complicate the model of the longitudinal-transverse deformation of the plate under preliminary tension by membrane forces and to solve problem (22) with variable coefficients.

Conclusion. The selected deformation model, as *a model of a flexible plate of small deflection* made of an orthogonal anisotropic material, makes it possible to solve the problems of ensuring the rigidity and strength of compound longitudinal-transverse bending of an orthotropic plate.

For a rectangular plate, according to the selected deformation model, in order to ensure a minimum deflection from a concentrated force, it is more advantageous to install fibers of a unidirectional composite along the short side. Stress levels and deflection are reduced.

Significant bending moments arising in the zone of application of a concentrated force are a source of stress concentration. The pre-tension of the plate web allows the stress to be reduced by 50 times.

The problem of compound bending of isotropic and anisotropic plates when applying transverse and selecting longitudinal loads with constraints on strength and stiffness can be called the problem of rational design of a structure. The obtained equations and the calculation program can be used both in the design of plate structures and in the educational process.

References

1. Morozov E. V., Lopatin A. V. Analysis and design of the flexible composite membrane stretched on the spacecraft solar array frame. *Composite Structures.* 2012, No. 94, P. 3106–3114.

2. Lopatin A. V., SHumkova L. V., Gantovnik V. B. *Nelineynaya deformaciya ortotropnoj membrany, rastyanutoj na zhestkoj rame solnechnogo elementa. V: Protokol 49 konferencii AIAA / ASME / ASCE / AHS / ASC, strukturnoj dinamiki i materialov, 16 konferencii AIAA / ASME / AHS po adaptivnym strukturam. 10t, Schaumburg, IL: AIAA-2008-2302* [Nonlinear deformation of an orthotropic membrane stretched on a rigid frame of a solar cell. In: Minutes of the 49th AIAA / ASME / ASCE / AHS / ASC Conference, Structural Dynamics and Materials, 16th AIAA / ASME / AHS Conference on Adaptive Structures. 10t, schaumburg, il: aiaa-2008-2302]. april 7–10, 2008.

3. Vasil'ev V. V., Protasov V. D., Bolotin V. V. et al. *Kompozicionnye materialy: Spravochnik* [Composite materials: handbook]. Moscow, Mashinostroenie Publ., 1990, 512 p.

4. Papkovich P. F. *Stroitel'naya mekhanika korablya. CHast' II. Slozhnyy izgib, ustojchivost' sterzhney i ustojchivost' plastin* [Construction mechanics of the ship. Part II. Complex bending, stability of rods and stability of plates]. Leningrad, Sudpromgiz Publ., 1941, 960 p.

5. Papkovich P. F. *Stroitel'naya mekhanika korablya* [Construction mechanics of the ship]. Vol. 1. Iss. 1. Moscow, Morskoy transport Publ., 1945, 618 p.

6. Lukasevich S. *Lokal'nye nagruzki v plastinah i obolochkah* [Local loads in plates and shells]. Moscow, Mir Publ., 1982, 544 p.

7. Novozhilov V. V. *Osnovy nelinejnoj teorii uprugosti* [Fundamentals of the nonlinear theory of elas-

ticity]. Leningrad – Moscow, OGIZ-Gostekhizdat Publ., 1948, 212 p.

8. Timoshenko S. P. *Ustoychivost' uprugih system* [Stability of elastic systems]. Leningrad – Moscow, OGIZ-Gostekhizdat Publ., 1946, 532 p.

9. Timoshenko S. P., Yung D. *Inzhenernaya mekhanika* [Engineering mechanics]. Moscow, Mashgiz Publ., 1960, 508 p.

10. Lyav A. *Matematicheskaya teoriya uprugosti* [Mathematical theory of elasticity]. Moscow, ONTI Publ., 1935.

11. Vol'mir A. S. *Gibkie plastinki i obolochki* [Flexible plates and shells]. Moscow, Gostekhizdat Publ., 1956, 419 p.

12. Il'yushin A. A., Lenskiy V. S. *Soprotivlenie materialov* [Resistance of materials]. Moscow, Fizmatgiz Publ., 1959, 372 p.

13. Kauderer G. *Nelineynaya mekhanika* [Nonlinear mechanics]. Moscow, Izd-vo inostrannoy literatury Publ., 1961, 778 p.

14. Lejbenzon L. S. *Kurs teorii uprugosti* [Course of the theory of elasticity]. Leningrad – Moscow, OGIZ Publ., 1947, 465 p.

15. Lukash P. A. *Osnovy nelineynoy stroitel'noy mekhaniki* [Fundamentals of nonlinear construction mechanics]. Moscow, Stroyizdat Publ., 1978, 204 p.

16. Novackij V. *Teoriya uprugosti* [Theory of elasticity]. Moscow, Mir Publ., 1975, 872 p.

17. Lekhnickiy S. G. *Teoriya uprugosti anizotropnogo tela* [Theory of elasticity of an anisotropic body]. Moscow, Nauka Publ., 1977, 416 p.

18. Samarskij A. A. *Teoriya raznostnyh skhem* [Theory of difference schemes]. Moscow, Nauka Publ., 1977, 656 p.

19. Govoruhin V., Cybulin V. *Komp'yuter v matematicheskom issledovanii. Uchebnyy kurs* [Computer in mathematical research: training course]. St. Petersburg, Piter Publ., 2001, 624 p.

Библиографические ссылки

1. Morozov E. V., Lopatin A. V. Analysis and design of the flexible composite membrane stretched on the spacecraft solar array frame // Composite Structures. 2012. No. 94. P. 3106–3114.

2. Лопатин А. В., Шумкова Л. В., Гантовник В. Б. Нелинейная деформация ортотропной мембраны, растянутой на жесткой раме солнечного элемента. В: Протокол 49-й конференции AIAA / ASME / ASCE / AHS / ASC, структурной динамики и материалов, 16-й конференции AIAA / ASME / AHS по адаптивным структурам. 10t, Schaumburg, IL: AIAA-2008-2302; 7–10 апреля 2008 г.

3. Композиционные материалы : справочник / В. В. Васильев, В. Д. Протасов, В. В. Болотин и др. М. : Машиностроение, 1990. 512 с.

4. Папкович П. Ф. Строительная механика корабля. Ч. II. Сложный изгиб, устойчивость стержней и устойчивость пластин. Ленинград : СУДПРОМГИЗ, 1941. 960 с.

5. Папкович П. Ф. Строительная механика корабля. Ч. 1. Т. 1. М. : Морской транспорт, 1945. 618 с.

6. Лукасевич С. Локальные нагрузки в пластинах и оболочках. М. : Мир, 1982. 544 с.

7. Новожилов В. В. Основы нелинейной теории упругости. Л.-М. : ОГИЗ-Гостехиздат. 1948. 212 с.

8. Тимошенко С. П. Устойчивость упругих систем. М.-Л. : ОГИЗ-Гостехиздат, 1946. 532 с.

9. Тимошенко С. П., Юнг Д. Инженерная механика. М. : Машгиз, 1960. 508 с.

10. Ляв А. Математическая теория упругости. М. : ОНТИ, 1935.

11. Вольмир А. С. Гибкие пластинки и оболочки. М. : Гостехиздат, 1956. 419 с.

12. Ильюшин А. А., Ленский В. С. Сопротивление материалов. М. : Физматгиз, 1959. 372 с.

13. Каудерер Г. Нелинейная механика. М. : Изд-во иностранной лит-ы, 1961. 778 с.

14. Лейбензон Л. С. Курс теории упругости. М.-Л. : ОГИЗ, 1947. 465 с.

15. Лукаш П. А. Основы нелинейной строительной механики. М. : Стройиздат, 1978. 204 с.

16. Новацкий В. Теория упругости. М. : Мир, 1975. 872 с.

17. Лехницкий С. Г. Теория упругости анизотропного тела. М. : Наука, 1977. 416 с.

18. Самарский А. А. Теория разностных схем. М. : Наука, 1977. 656 с.

19. Говорухин В., Цыбулин В. Компьютер в математическом исследовании : учебный курс. СПб. : Питер, 2001. 624 с.

Rashid Altavovich Sabirov – Ph. D., Associate Professor; Reshetnev Siberian State University of Science and Technology. E-mail: rashidsab@mail.ru.

Сабиров Рашид Альтавович – кандидат технических наук, доцент, доцент кафедры технической механики; Сибирский государственный университет науки и технологий имени академика М. Ф. Решетнева. E-mail: rashidsab@mail.ru.